Influence of the isovector-scalar channel interaction on neutron star matter with hyperons and antikaon condensation

Guo-yun Shao (邵国运)[1,2] and Yu-xin Liu (刘玉鑫)[1,3,*]

[1]*Department of Physics and State Key Laboratory of Nuclear Physics and Technology, Peking University, Beijing 100871, China*

[2]*INFN-Laboratori Nazionali del Sud, Via S. Sofia 62, I-95125 Catania, Italy*

[3]*Center of Theoretical Nuclear Physics, National Laboratory of Heavy Ion Accelerator, Lanzhou 730000, China*

(Received 15 September 2010; published 4 November 2010)

The relativistic mean field approach including isovector-scalar channel (i.e., exchanging δ mesons) interaction is taken to study the properties of neutron star matter including hyperons and antikaon condensation. For hyperonic neutron stars, it shows that the δ-meson channel interaction stiffens the equation of state at lower densities but it softens the equation of state after hyperons appear. This leads to the neutron star having a lower central density and a larger radius than the one with the same mass but without the δ-meson channel interaction. For neutron star matter including both hyperons and antikaon condensation, the δ-meson channel interaction increases the onset density of the antikaon condensation. At the same time, the stability of the kaonic neutron star and its dependence on the kaon optical potential are discussed. For stable kaonic neutron stars with larger radii, those with the inclusion of the δ-meson channel interaction have larger masses than those without the δ-meson interaction, but the result is reversed for those with smaller radii. Calculated results are also compared with neutron star observations. Constraints on the model parameters are then provided.

DOI: 10.1103/PhysRevC.82.055801 PACS number(s): 26.60.Kp, 97.60.Jd, 21.30.Fe, 21.65.Cd

I. INTRODUCTION

Because the density in the core range of a neutron star may be several times the nuclear saturation density (ρ_0), the conventional view of neutron star matter composed of protons, neutrons, and electrons is insufficient and more realistic compositions are needed (for recent reviews, see, e.g., Refs. [1] and [2]). At high densities, some new degrees of freedom such as hyperons [3–9], condensed (anti)kaons [10–25], Δ isobars [26–29], and quarks [30–40] can possibly appear. Moreover, particles with strangeness, such as (anti)kaons and hyperons, are created through strong and weak reactions until chemical equilibrium is reached. All populations are distributed among different species so as to account for the lowest energy state of neutron star matter under the constraint of β equilibrium and charge neutrality.

The possibility of the appearance of (anti)kaon condensation in hyperonic neutron star matter and its effect have been discussed for a long time (see, e.g., Refs. [3] and [41]). In the interior of neutron stars, the chemical potential of electrons increases, and the effective mass of K^- mesons decreases with an increase in baryon density. As the effective mass of the mesons is reduced to the critical mass equating to the chemical potential of electrons, negatively charged kaons, being bosons, are able to condense in the lowest momentum ($k = 0$) state [11]. At densities higher than the threshold, negative kaons will replace electrons as the neutralizing agent, and the electron population may be quenched by the quick increase in negative kaons. This scenario was first demonstrated clearly by Kaplan and Nelson with a chiral Lagrangian model; they showed that K^- mesons may undergo Bose-Einstein condensation in dense hadronic matter [41]. Later, such a composition of the core of neutron stars was studied more systematically in the chiral model [42–44]. In Refs. [45] and [46], kaon condensation was investigated further in the traditional meson-exchange picture in the framework of the relativistic mean field (RMF) model. Glendenning and Schaffner studied in detail first-order kaon condensation in the interior of neutron stars in the absence of hyperons with the Gibbs criteria for more than one conserved charge [11]. There are also relevant investigations of kaon condensation using other models, such as the (modified) quark-meson coupling model [15,22,47] and the density-dependent RMF model from microscopic Dirac-Brueckner calculations with the Groningen and Bonn potential of nucleon-nucleon interaction [48,49]. All these calculations indicate that the inclusion of negatively charged kaons softens the equation of state (EOS) of the matter and, in turn, reduces the maximum mass of neutron stars determined by the Tolman-Oppenheimer-Volkoff (TOV) equation [50,51].

Furthermore, Brown and collaborators [17,52–54] claimed that kaon condensation is the most likely phase transition in the interior of neutron stars and the onset of antikaon condensation will send neutron stars into low-mass black holes. This was also applied to explain the disappearance of the neutron star created in SN1987A after it had emitted neutrinos for about 12 s [54]. With such a phase transition, Brown's scenario also predicted that there are about 5 times more low-mass black hole/neutron star binaries than neutron star/neutron star binaries (details are given in Ref. [54]). Some simulations of the evolution of a proto-neutron star with kaon-condensed matter have also been presented [55]. It is thus a very interesting issue to investigate the stability of neutron stars with the inclusion of kaon condensation.

*yxliu@pku.edu.cn

Concerning the theoretical approaches, we have known that the RMF approximation of quantum hadron dynamics is a simple and successful method for describing the properties of nuclei and nuclear matter [56,57]. In the commonly used RMF approach, the baryon-baryon interaction is realized by exchanging the isoscalar-scalar σ meson, isoscalar-vector ω meson, and isovector-vector ρ meson. In addition, self-couplings between the respective mesons have been taken into account [58–60]. In recent years, meson-meson cross-interactions between different meson species have also been included to describe finite nuclei, nuclear matter, and neutron stars better [60–65].

In general point of view, there exists isovector-scalar channel (exchanging δ mesons) interaction between baryons. Some studies have then been carried out to investigate its effect using the RMF approach (see, e.,g., Refs. [24], [48], and [66]–[72]). It has been shown that such an interaction plays an important role in neutron skins, pygmy resonances, nuclear structure at the drip line, neutron distillation in fragmentation, the EOS of isospin asymmetric nuclear matter at low densities, and so forth [70–72]. The effect of the δ-meson channel interaction on some properties of neutron stars with (anti)kaon condensation has also been discussed [24,48]. It is shown that the inclusion of δ-meson channel interaction shifts the onset density of K^- condensation to a higher one, which, in turn, affects the EOS of neutron star matter [24]. However, hyperons were not taken into account in Ref. [24], for simplicity. Theoretically, if one considers antikaon mesons composed of strange quark flavors, it is necessary to include hyperons in consideration of β equilibrium. This case was studied in Ref. [48], where two different parameter sets, Groningen and Bonn A, are used. However, the δ-meson channel interaction is only included in the former parameter set, and the parameters are taken with completely different values in the two cases. So the role of the δ-meson channel interaction has not yet been demonstrated clearly. Moreover, the model parameters taken in Ref. [48] should be investigated as suggested by Cescato and Ring [73] because they give rise to a negative effective nucleon mass at high densities.

The main purpose of this paper is thus to study the effect of the δ-meson channel interaction on the properties of neutron stars with both hyperons and (anti)kaon condensation, using different parameter sets. Some relevant works [23,24] have not considered hyperon degrees of freedom. In Ref. [24] we focused particularly on comparison of the role of the δ-meson channel interaction in different models, such as the Glendenning-Moszkowski (GM) [74], the Zimanyi-Moszkowski [75], and the hybrid derivative coupling models [76], which handle the scalar meson field dependence of the effective mass of nucleons in different ways, and found that the differences among the three models are very small. Therefore, here we consider the matter including both hyperons and kaon condensation only in the GM model. In this paper, as a continuation and extension of Ref. [24], we also analyze the stability of neutron stars and compare the theoretical result with some astronomical observations and, thus, provide constraints on the theoretical model.

The paper is organized as follows. In Sec. II, we briefly describe the effective Lagrangian and give the relevant formulas in the RMF theory. In Sec. III, we demonstrate the calculated properties of neutron stars including hyperons and kaon condensation with and without the δ-meson channel interaction. In addition, we present some observation constraints on the model parameters. Finally, a summary is given in Sec. IV.

II. THE MODEL

The RMF approach has been widely implemented to describe the properties of hadronic matter and finite nuclei, in which baryons interact via the exchange of mesons. We consider here the whole baryon octet including both nucleons (p and n) and hyperons (Λ, Σ, and Ξ) that was first investigated by Glendenning [77]. The mesons exchanged include not only the isoscalar-scalar meson (σ), isoscalar-vector meson (ω), and isovector-vector meson (ρ) but also the isovector-scalar meson (δ). For neutron star matter with the entire baryon octet and negatively charged leptons, the effective Lagrangian can be written as

$$\begin{aligned}\mathcal{L} = \sum_B \bar{\Psi}_B \Big[& i\gamma_\mu \partial^\mu - m_B + g_{\sigma B}\sigma + \frac{1}{2} g_{\delta B} \boldsymbol{\tau}_B \cdot \boldsymbol{\delta} - g_{\omega B}\gamma_\mu \omega^\mu \\ & - \frac{1}{2} g_{\rho B}\gamma_\mu \boldsymbol{\tau}_B \cdot \boldsymbol{\rho}^\mu \Big] \Psi_B + \frac{1}{2}\left(\partial_\mu \sigma \partial^\mu \sigma - m_\sigma^2 \sigma^2\right) \\ & - \frac{1}{3} b\, m (g_\sigma \sigma)^3 - \frac{1}{4} c\, (g_\sigma \sigma)^4 + \frac{1}{2}\left(\partial_\mu \delta \partial^\mu \delta - m_\delta^2 \delta^2\right) \\ & + \frac{1}{2} m_\omega^2 \omega_\mu \omega^\mu - \frac{1}{4}\omega_{\mu\nu}\omega^{\mu\nu} + \frac{1}{2} m_\rho^2 \boldsymbol{\rho}_\mu \cdot \boldsymbol{\rho}^\mu \\ & - \frac{1}{4}\boldsymbol{\rho}_{\mu\nu} \cdot \boldsymbol{\rho}^{\mu\nu} + \sum_\ell \bar{\Psi}_\ell (i\gamma_\mu \partial^\mu - m_\ell)\Psi_\ell, \end{aligned} \tag{1}$$

where the subscript B stands for the entire baryon octet (p, n, Λ, Σ^+, Σ^0, Σ^-, Ξ^0, Ξ^-) and ℓ represents charged leptons e^- and μ^-. m_B, m_σ, m_δ, m_ω, and m_ρ are masses assigned to the corresponding baryons and mesons. $g_{\sigma B}$, $g_{\omega B}$, $g_{\delta B}$, $g_{\rho B}$, b, and c refer to the meson-baryon or meson-meson (self-)coupling constants. The antisymmetric tensors of vector mesons are given by

$$\omega_{\mu\nu} = \partial_\mu \omega_\nu - \partial_\nu \omega_\mu, \quad \boldsymbol{\rho}_{\mu\nu} \equiv \partial_\mu \boldsymbol{\rho}_\nu - \partial_\nu \boldsymbol{\rho}_\mu.$$

With the mean field approximation, by which the operators of meson fields are replaced by their expectation values, we can obtain the meson field equations as

$$g_{\sigma N}\sigma = f_\sigma \left[\sum_B x_{\sigma B} \rho_B^S - bm(g_{\sigma N}\sigma)^2 - c(g_{\sigma N}\sigma)^3 \right], \tag{2}$$

$$g_{\delta N}\delta = f_\delta \sum_B x_{\delta B} I_{3B} \rho_B^S, \tag{3}$$

$$g_{\omega N}\omega = f_\omega \sum_B x_{\omega B} \rho_B, \tag{4}$$

$$g_{\rho N}\rho = f_\rho \sum_B x_{\rho B} I_{3B} \rho_B, \tag{5}$$

where new forms of coupling constants are adopted with the definitions

$$f_i = \left(\frac{g_{iN}}{m_i}\right)^2, \quad x_{iB} = \frac{g_{iB}}{g_{iN}} \quad (i = \sigma, \delta, \omega, \rho),$$

and ρ_B and ρ_B^S are the baryon density and the scalar density, respectively, with

$$\rho_B = \frac{1}{\pi^2}\int_0^{k_F^B} k^2 dk, \tag{6}$$

$$\rho_B^S = \frac{1}{\pi^2}\int_0^{k_F^B} k^2 dk \frac{m_B^*}{\sqrt{k^2+m_B^{*2}}}. \tag{7}$$

In the last two equations, k_F^B is the Fermi momentum of baryon B, and m_B^* is the corresponding effective mass in the nuclear medium with

$$m_B^* = m_B - g_{\sigma B}\sigma - \tfrac{1}{2} g_{\delta B}\tau_{3B}\delta. \tag{8}$$

With the requirement of translational invariance and rotational symmetry of static, homogeneous, infinite nuclear matter, besides the scalars σ and δ, only zero components—ω_0 and ρ_0—of the vector fields survive, which are denoted ω and ρ in the preceding meson equations.

For neutron star matter with baryons and charged leptons, the β-equilibrium condition is guaranteed with the following relations of chemical potentials for different particles:

$$\mu_p = \mu_{\Sigma^+} = \mu_n - \mu_{e^-}, \tag{9}$$

$$\mu_\Lambda = \mu_{\Sigma^0} = \mu_{\Xi^0} = \mu_n, \tag{10}$$

$$\mu_{\Sigma^-} = \mu_{\Xi^-} = \mu_n + \mu_{e^-}, \tag{11}$$

$$\mu_\mu = \mu_{e^-}. \tag{12}$$

And the charge-neutrality condition is fulfilled by

$$n_p + n_{\Sigma^+} = n_{e^-} + n_{\mu^-} + n_{\Sigma^-} + n_{\Xi^-}, \tag{13}$$

where n_i is the number density of species i. The chemical potentials of baryons and leptons are expressed by

$$\mu_B = \sqrt{k_F^{B^2} + m_B^{*^2}} + g_{\omega B}\omega + g_{\rho B} I_{3B}\rho, \tag{14}$$

$$\mu_\ell = \sqrt{k_{F,\ell}^2 + m_\ell^2}, \tag{15}$$

where $k_{F,\ell}$ and m_ℓ are the Fermi momentum and the mass of the lepton ℓ, respectively. The total energy density and the pressure of the neutron star matter are then written as

$$\begin{aligned}\varepsilon_N = {} & \sum_{i=B,\ell}\frac{2}{(2\pi)^3}\int d^3k\sqrt{k^2+m_i^{*2}} + \frac{1}{2}m_\sigma^2\sigma^2 \\ & + \frac{b}{3}m(g_{\sigma N}\sigma)^3 + \frac{c}{4}(g_{\sigma N}\sigma)^4 + \frac{1}{2}m_\delta^2\delta^2 \\ & + \frac{1}{2}m_\omega^2\omega^2 + \frac{1}{2}m_\rho^2\rho^2,\end{aligned} \tag{16}$$

$$\begin{aligned}p_N = {} & \sum_{i=B,\ell}\frac{1}{3}\frac{2}{(2\pi)^3}\int d^3k\frac{k^2}{\sqrt{k^2+m_i^{*2}}} - \frac{1}{2}m_\sigma^2\sigma^2 \\ & - \frac{b}{3}m(g_{\sigma N}\sigma)^3 - \frac{c}{4}(g_{\sigma N}\sigma)^4 - \frac{1}{2}m_\delta^2\delta^2 \\ & + \frac{1}{2}m_\omega^2\omega^2 + \frac{1}{2}m_\rho^2\rho^2.\end{aligned} \tag{17}$$

In the following, we denote this phase the normal phase.

With the onset of kaon condensation at higher densities, kaon-meson interactions should be taken into account, which are also mediated by σ, δ, ω, and ρ mesons in this model. With the minimal coupling scheme, $D_\mu = \partial_\mu + i g_{\omega K}\omega_\mu + i g_{\rho K}\tau_K\rho_\mu/2$, the following Lagrangian density describing the kaon-kaon interaction should be added to Eq. (1):

$$\mathcal{L}_K = D_\mu^*\bar{K} D_\mu K - m_K^*\bar{K}K, \tag{18}$$

where m_K^* is the effective mass of kaon meson in the medium and can be given explicitly as

$$m_K^* = m_K - g_{\sigma K}\sigma - \tfrac{1}{2}g_{\delta K}\tau_{3\bar{K}}\delta. \tag{19}$$

The isospin doublet for antikaons is $\bar{K} \equiv (\bar{K}^0,\ K^-)$, with the isospin projector $\tau_{3\bar{K}} = (+1,\ -1)$ for $\bar{K}^0$ and K^-, respectively. In the interior of neutron stars, the medium-modified kaon energy is reduced from its vacuum value to a lower, density-dependent one with the dispersion relation

$$\omega_{\bar{K}} = m_K^* - g_{\omega K}\omega + \tfrac{1}{2}g_{\rho K}\tau_{3\bar{K}}\rho. \tag{20}$$

At the same time, the electron chemical potential μ_{e^-} increases with increasing baryon density. As ω_{K^-} decreases to a certain threshold $\mu_{K^-} = \mu_{e^-}$, K^- mesons begin to show up in neutron star matter. In the following we denote this phase the kaon condensation phase.

For the kaon condensation phase, the meson field equations are modified as

$$\begin{aligned}(g_{\sigma N}\sigma)_{\bar{K}} = f_\sigma\Bigg[& \sum_B x_{\sigma B}\rho_B^S - bm(g_{\sigma N}\sigma)_{\bar{K}}^2 \\ & - c(g_{\sigma N}\sigma)_{\bar{K}}^3 + x_{\sigma K}\sum_{\bar{K}} n_{\bar{K}}\Bigg],\end{aligned} \tag{21}$$

$$(g_{\delta N}\delta)_{\bar{K}} = f_\delta\left[\sum_B x_{\delta B} I_{3B}\rho_B^S + x_{\delta K}\sum_{\bar{K}} I_{3\bar{K}} n_{\bar{K}}\right], \tag{22}$$

$$(g_{\omega N}\omega)_{\bar{K}} = f_\omega\left[\sum_B x_{\omega B}\rho_B - x_{\omega K}\sum_{\bar{K}} n_{\bar{K}}\right], \tag{23}$$

$$(g_{\rho N}\rho)_{\bar{K}} = f_\rho\left[\sum_B x_{\rho B} I_{3B}\rho_B + x_{\rho K}\sum_{\bar{K}} I_{3\bar{K}} n_{\bar{K}}\right], \tag{24}$$

where $x_{iK} = \frac{g_{iK}}{g_{iN}}$ $(i = \sigma, \delta, \omega, \rho)$. Because (anti)kaons are bosons, their condensation does not contribute to the pressure, the pressure of kaon phase has then the same form as that of the normal phase, i.e. Eq. (17), and

$$P_K(\mu_n,\ \mu_e) = P_N(\mu_n,\ \mu_e) \tag{25}$$

is required for the phase in which both the normal phase and the kaon condensation phase are in equilibrium (this phase is usually referred to as the mixed phase). However, the condensed kaon mesons contribute to the energy density of the kaon phase as

$$\begin{aligned}\varepsilon_K = {} & \sum_{i=B,\ell}\frac{2}{(2\pi)^3}\int_0^{k_F^i} d^3k\sqrt{k^2+m_i^{*2}} + \frac{1}{2}m_\sigma^2\sigma_{\bar{K}}^2 \\ & + \frac{b}{3}m(g_{\sigma N}\sigma)_{\bar{K}}^3 + \frac{c}{4}(g_{\sigma N}\sigma)_{\bar{K}}^4 + \frac{1}{2}m_\delta^2\delta_{\bar{K}}^2 + \frac{1}{2}m_\omega^2\omega_{\bar{K}}^2 \\ & + \frac{1}{2}m_\rho^2\rho_{\bar{K}}^2 + m_K^*\sum_{\bar{K}} n_{\bar{K}}.\end{aligned} \tag{26}$$

Because there are two conserved charges in the mixed phase, the baryon charge and the electric charge, the Maxwell construction, which produces the discontinuity of the energy and electron chemical potential in the interior of neutron star, is not feasible. The Gibbs conditions are usually implemented to describe the mixed phase, requiring all the chemical potentials, temperature, and pressure to be common to both phases in equilibrium [11]. This means that the kaon condensation phase occupies just a small fraction of the total volume of the system at the beginning of kaon condensation, and the proportion increases with increasing baryon density. The pure kaon condensation phase (including, of course, baryons, owing to chemical equilibrium) may be reached finally. In the mixed phase, the conservation of electric charge is satisfied globally by the combination of the two phases, not locally by one single phase, which can be explicitly written as

$$q_{\text{total}} = \chi q_K(\mu_n,\ \mu_e) + (1-\chi)\, q_N(\mu_n,\ \mu_e) = 0, \quad (27)$$

where χ is the volume fraction of the kaon condensation phase, and q_K and q_N denote the electric charge density of the kaon condensation phase and the normal phase, respectively.

With the obtained EOS of the neutron star matter, the mass-radius relation and other relevant quantities of the neutron star can be derived by solving the TOV equation [50,51],

$$\frac{dp}{dr} = \frac{[p(r)+\epsilon(r)][M(r)+4\pi r^3 p(r)]}{r[r-2M(r)]}, \quad (28)$$

with

$$M(r) = 4\pi \int_0^R \epsilon(r) r^2 dr. \quad (29)$$

The equations of motion of the hadrons involve six parameters, f_σ, f_δ, f_ω, f_ρ, b, and c, which can be determined by the Bonn potential and the bulk properties of the nuclear matter at saturation density. The value of f_δ in this paper is 4 times that used in some studies (e.g., Refs. [66], [67], and [78]), owing to the different expressions of the isospin operator, so for consistency we choose $f_\delta = 2.5$ and $f_\delta = 10.0$, which correspond to Bonn potentials A and C, respectively [78]. Of the properties of nuclear matter at saturation density, the best known are the binding energy and the symmetry energy coefficient, while the effective nucleon mass and the compression modulus are not well fixed. Therefore, here several sets of the bulk properties of nuclear matter are adopted from Refs. [57] and [74]: (a) GM1, with $\rho_0 = 0.153$ fm^{-3}, $E/A = -16.3$ MeV, $a_{\text{asym}} = 32.5$ MeV, $K = 300$ MeV, and $m^* = 0.7$ m; (b) GM2, with $\rho_0 = 0.153$ fm^{-3}, $E/A = -16.3$ MeV, $a_{\text{asym}} = 32.5$ MeV, $K = 300$ MeV, and $m^* = 0.78$ m; and (c) GM3, with $\rho_0 = 0.153$ fm^{-3}, $E/A = -16.3$ MeV, $a_{\text{asym}} = 32.5$ MeV, $K = 240$ MeV, and $m^* = 0.78$ m. The fitted results of the model parameters are listed in Table I. The different choices of model parameters will demonstrate different neutron star structures, which may inversely put constraints on the nuclear matter properties at saturation density by accurate neutron star observation.

Meson-hyperon and meson-kaon coupling constants relevant to ω, ρ, and δ mesons are taken from the SU(6) quark model, with

$$\begin{aligned} g_{\omega\Lambda} &= g_{\omega\Sigma} = 2g_{\omega\Xi} = 2g_{\omega N}/3, \\ g_{\rho\Lambda} &= 0, \quad g_{\rho\Sigma} = 2g_{\rho\Xi} = 2g_{\rho N}, \\ g_{\delta\Lambda} &= 0, \quad g_{\delta\Sigma} = 2g_{\delta\Xi} = 2g_{\delta N}, \\ g_{\rho K} &= g_{\rho N}, \quad g_{\omega K} = g_{\omega N}/3. \end{aligned} \quad (30)$$

As for the couplings of σ mesons, they can be obtained by fitting hyperon potentials with $U_Y^N = x_{\omega Y} V - x_{\sigma Y} S$, where $S = g_\sigma \sigma$ and $V = g_\omega \omega$ are the values of the scalar and vector field strengths at saturation density [74,79]. The Λ-N interaction has been well studied and $U_\Lambda^N = -28$ MeV was obtained with bound Λ hypernuclear states (see, e.g., Ref. [80]). However, at present the Σ-N interaction in nuclear matter is not known clearly. If Σ were bounded in nuclear matter [7,81], the attractive potential should be used, but detailed scans for Σ hypernuclear states turned out to give negative results [82,83]. The study of Σ^- atoms also showed strong evidence for a sizable repulsive potential in the nuclear core at $\rho = \rho_0$ [84,85] and this was confirmed by a new geometric analysis of the Σ^- atom data [86]. Therefore, here we take $U_\Sigma^N = 30$ MeV as used in Refs. [80] and [87] to fix the parameter $\chi_{\sigma\Sigma}$. In addition, the Ξ-N interaction is attractive, with the potential $U_\Xi^N = -18$ MeV [80,87]. Scalar meson coupling to K^- mesons is obtained by fitting the kaon optical potential with $U_K = -g_{\sigma K}\sigma - g_{\omega K}\omega$ at the saturation density of nuclear matter. Fits to kaonic atom data have yielded values of U_K in the range of -50 to -200 MeV [86,88–93].

TABLE I. Parameters used in our calculations by fitting the saturation properties of nuclear matter. $f_\delta = 2.5$ and $f_\delta = 10.0$ correspond approximately to Bonn potential A and potential C, respectively [78].

	f_σ	f_ω	f_ρ	b	c
GM1					
No δ	11.7935	7.158 73	4.413 61	0.002 94	−0.001 07
$f_\delta = 2.5$	11.7935	7.158 73	6.572 29	0.002 94	−0.001 07
$f_\delta = 10.0$	11.7935	7.158 73	12.989 52	0.002 94	−0.001 07
GM2					
No δ	9.153 87	4.828 03	4.793 87	0.003 48	0.013 19
$f_\delta = 2.5$	9.153 87	4.828 03	7.011 89	0.003 48	0.013 19
$f_\delta = 10.0$	9.153 87	4.828 03	13.620 89	0.003 48	0.013 19
GM3					
No δ	9.932 30	4.828 03	4.793 87	0.008 63	−0.002 43
$f_\delta = 2.5$	9.932 30	4.828 03	7.011 89	0.008 63	−0.002 43
$f_\delta = 10.0$	9.932 30	4.828 03	13.620 89	0.008 63	−0.002 43

III. NUMERICAL RESULT AND DISCUSSION

A. Effect of the δ-meson channel interaction on neutron stars with hyperons

Before taking into account neutron star matter with kaon condensation, we first simply investigate the properties of neutron stars with the presence of only nucleons and hyperons for convenience of comparison. In Ref. [65], the neutron star with hyperons was studied with and without the δ-meson

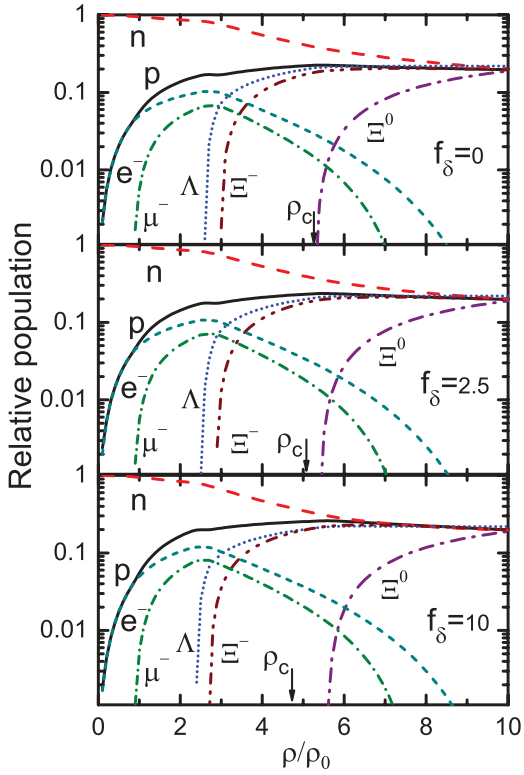

FIG. 1. (Color online) Calculated variation behaviors of the relative populations in the composition of a neutron star with respect to the total baryon density using parameter set GM2. The upper panel is the result without the δ-meson channel interaction. The middle and lower panels are those including the δ-meson channel interaction. ρ_c denotes the density at the center of the neutron star.

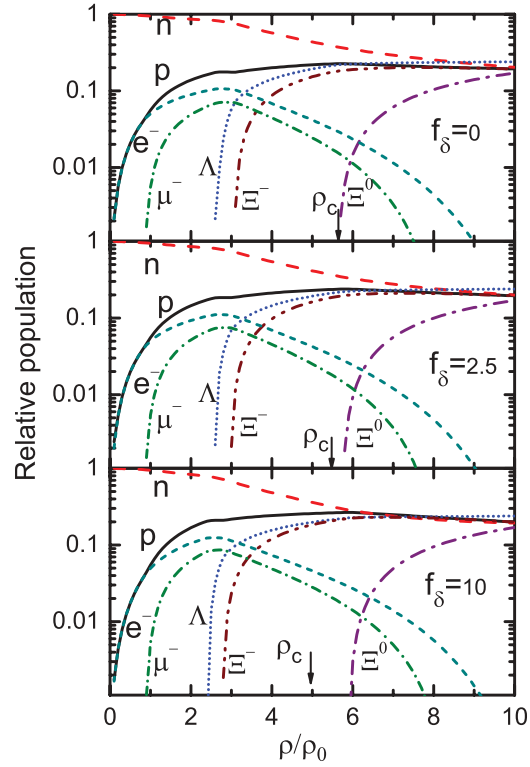

FIG. 2. (Color online) The same as Fig. 1 but using parameter set GM3.

channel interaction, but only the mass-radius relation was reported there. How the δ-meson channel interaction affects the inner structure of the star remains to be explored. We thus focus mainly on this subject here.

With the parameters listed in Table I, we obtain the relative populations of all species including both baryons and leptons. The results are presented in Fig. 1 for the parameter set GM2 and in Fig. 2 for GM3. In these figures, the upper panels display the results without the δ-meson channel interaction, and the middle and lower panels show the results including the δ-meson channel interaction. Figures 1 and 2 apparently show that Σ hyperons do not appear in the interior of neutron stars, as the potential U_Σ^N is repulsive. If the parameter f_δ takes a small value, $f_\delta = 2.5$, its influence on the population distribution is almost negligible. However, if f_δ takes a larger value, for instance, f_δ =10, it affects the onset densities of hyperons obviously, especially those of the isospin doublet Ξ^0 and Ξ^-, with the onset of Ξ^- being shifted to a lower density and that of Ξ^0 to a higher one. The shifted densities are about $0.3\rho_0$.

With the solutions of the field equations of baryons and mesons, we can directly obtain the EOS of the system. The results obtained with several sets of parameters are illustrated in Fig. 3. First, by comparing the results with the parameter sets GM1, GM2, and GM3, we find that a larger compression modulus and a smaller effective nucleon mass at saturation density give a stiffer EOS. Furthermore, for each parameter set, inclusion of the δ-meson channel interaction causes the EOS of the matter at low densities to be harder but the EOS at high densities to be softer, and hyperons lower the density at which the EOS becomes softer. Specifically, such a change in the EOS from stiffness to softness takes place

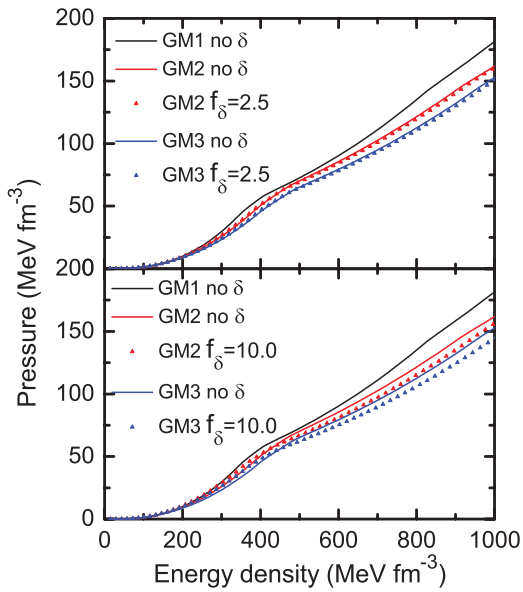

FIG. 3. (Color online) Calculated equations of state of hyperonic neutron star matter for parameter sets GM1, GM2, and GM3. Solid curves are the results without the δ-meson channel interaction, and dotted curves are those including that channel interaction.

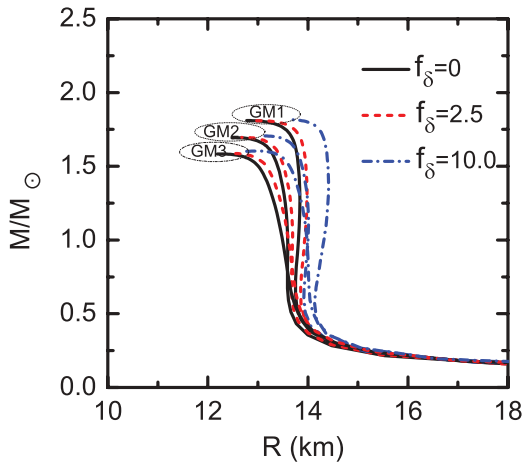

FIG. 4. (Color online) Calculated mass-radius relations of hyperonic neutron stars for parameter sets GM1, GM2, and GM3. Solid curves are the results without the δ-meson channel interaction, and dashed and dot-dashed curves are those with the δ-meson channel interaction.

when the energy density is in the region of 400–500 MeV fm^{-3} for different parameter sets. However, for a simple neutron star whose baryon composition includes only neutrons and protons, the change begins at a relatively higher energy density, with $\varepsilon > 950$ MeV fm^{-3}. Comparing these features, one can confirm that the δ-meson channel interaction makes the EOS of the matter harder and hyperons soften the EOS. Because of this competition, the EOS of the matter at low densities at which hyperons do not appear becomes stiffer. This characteristic of the EOS influences the central density of neutron stars. For example, with the parameter set GM3, a star with a maximum mass without hyperons and without the δ-meson channel interaction has a central density of 7.1 ρ_0, but this decreases to 6.8 ρ_0 when the δ-meson channel interaction with $f_\delta = 10.0$ is included. For the same parameter set, GM3, the central density of stars including hyperons are correspondingly 5.7 ρ_0 and 4.9 ρ_0 for the two cases without and with the δ-meson channel interaction. Combining the results in Figs. 1 and 2, we conclude that the central density of neutron stars is reduced with the inclusion of the δ-meson channel interaction.

We also illustrate the calculated results for the mass-radius relation of hyperonic neutron stars in Fig. 4. The specific values of the maximum masses and the radii of hyperonic neutron stars with the three sets of parameters are listed in Table II. Combining the results shown in Figs. 3 and 4 for parameter sets GM1, GM2, and GM3, we find that a stiffer EOS produces a larger maximum mass of neutron stars. Moreover, for each parameter set, the difference between the maximum mass of a neutron star with the inclusion of the δ-meson channel interaction and that without the δ-meson channel interaction is very small, but the radius of a neutron star with the δ-meson channel interaction is much larger than that without the δ mesons.

TABLE II. Calculated results of the maximum masses and radii of hyperonic neutron stars for the three sets of parameters. (The ones marked with "with δ" are those obtained with $f_\delta = 10.0$).

	GM1		GM2		GM3	
	No δ	With δ	No δ	With δ	No δ	With δ
$M_{\max}$ ($M_\odot$)	1.81	1.82	1.69	1.71	1.58	1.60
R (km)	12.82	13.58	12.55	13.13	12.22	12.95

To understand the effect of the δ-meson channel interaction on the properties of neutron stars including hyperons, we use the EOS of hyperonic neutron star matter. As already mentioned, the δ-meson channel interaction only stiffens the EOS of the matter at low densities, and softens the EOS at high densities at which hyperons emerge, and the density and pressure at the center of neutron stars are smaller than the respective values in the case without the δ-meson channel interaction. The lower density and pressure at the center of a neutron star show that the gravity in the center region of the star is weak, owing to the requirement for mechanical stability. At first glance it seems that a neutron star with the δ-meson channel interaction should thus have a small radius. However, as a matter of fact, because the EOS at lower densities of the matter is harder as the δ-meson channel interaction is taken into account, it can thus resist stronger gravity from the outer layer of the star. Therefore, as the profile of the matter displayed in Fig. 5 shows, the outer layer of a neutron star with the inclusion of the δ-meson channel interaction is thicker than that of a neutron star without δ mesons. In contrast, the softness of the EOS at higher densities with the inclusion of δ mesons reduces the central density of the star. As a consequence, a neutron star composing matter with the δ-meson channel interaction can have a relatively larger radius than the one with the same mass but without the δ-meson channel interaction. In fact, Ref. [69] reported a similar result, except that the smallest

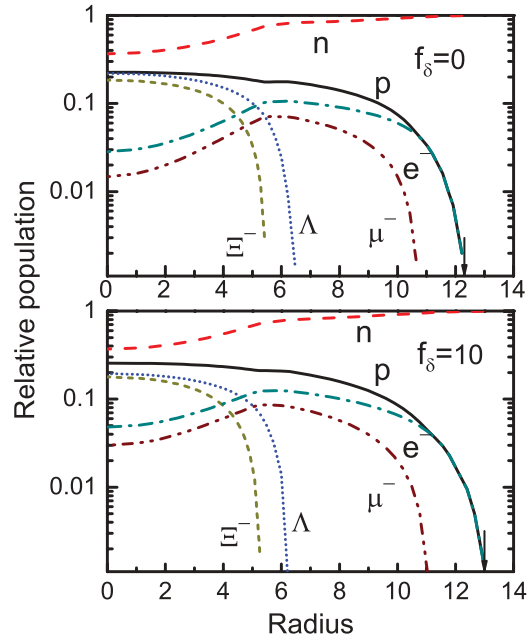

FIG. 5. (Color online) Calculated matter profiles of hyperonic neutron stars for parameter set GM3. The upper panel shows profiles without the δ-meson channel interaction; the lower panel displays those including the interaction with parameter $f_\delta = 10$.

radius of a neutron star obtained there was smaller than ours, owing to the different choice of model parameters, especially meson-hyperon interaction constants. The relevant parameters in the present work are taken from the SU(6) quark model, but those in Ref. [69] are taken by assumption.

To sum up, inclusion of the δ-meson channel interaction may exert a great influence on the properties of hyperonic neutron stars such as the population distribution of baryons and the mass-radius relation. However, the result depends on the coupling strength between δ meson and nucleon. Unfortunately, to date, experiments have not provided enough information about this. We hope that heavy-ion reactions will provide us a chance to investigate the isospin effect directly [71] in the near-future.

B. Effect of the δ-meson channel interaction on kaonic neutron stars

In this subsection we study the properties of neutron star matter with both kaon condensation and hyperons. Considering the fact that the K^- meson begins condensing at a lower density than other kaon species because its effective mass is smaller in nuclear medium [94], and it is favored as the neutralizing agent of positive electric charge, we take only K^- mesons into account here. Because Σ hyperons do not appear in neutron star matter in the case of a repulsive potential (see the preceding result and that given in Ref. [9]), and Ξ^0 hyperons emerge at a density higher than the central density of hyperonic neutron stars as the δ-meson channel interaction is included, we do not consider these hyperons in our calculation.

As for the parameter f_δ, it has been shown that $f_\delta = 2.5$ and $f_\delta = 10$ correspond to Bonn potentials A and C, respectively [78]. In Ref. [24], $f_\delta = 10$ was used to study antikaon condensation in the case without hyperons. In this paper, we intended to take both $f_\delta = 10$ and $f_\delta = 2.5$ to discuss the effect of the δ-meson channel interaction strength on neutron stars (matter) with both antikaon condensation and hyperons. In the calculation, 11 coupled equations are being solved simultaneously. If $f_\delta = 10$ is used, solutions for the coupled equations when both hyperons and antikaon condensation are considered at the same time do not exist. As we lower the value of f_δ, we note that, even at $f_\delta = 8$, solutions exist only for some parameter sets. So, to make sure we can always find solutions with the different parameter sets, we take the intermediate value $f_\delta = 4$, between Bonn potential A and Bonn potential C. It is also difficult to fix the value of $x_{\delta K}$ from nuclear experiments at present. In the calculation, we find that its value cannot be too large to ensure the existence of solutions. For example, solutions can only be found with $x_{\delta K} < 0.3$ for parameter set GM1 with $U_K = -160$ MeV. Here we thus take only the value $x_{\delta K} = 0.2$ for all parameter sets. In addition, by comparing the parameter sets and the results given in Sec. III A, we can note that parameter set GM1 is different from GM3 for both the effective nucleon mass and the compression modulus of the matter, and they provide a bigger difference in the EOS and the mass-radius relation; we thus use these two parameter sets to study the properties of kaonic neutron stars in the following.

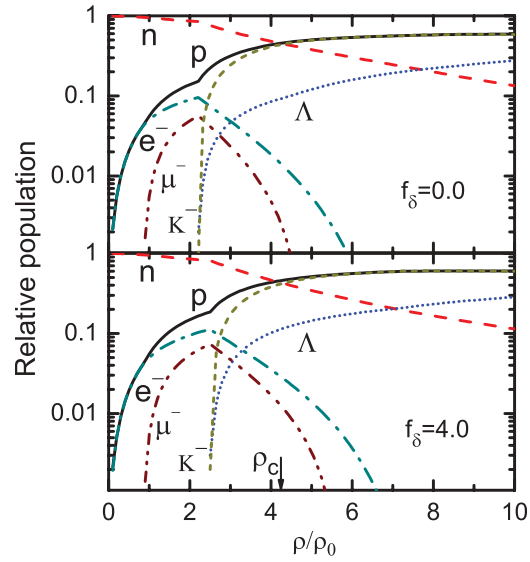

FIG. 6. (Color online) Calculated variation behaviors of the relative populations of all compositions of neutron stars with respect to the baryon density using parameter set GM3 and $U_K = -130$ MeV.

By solving the field equations with the Gibbs criteria for equilibrium of phases, we get the relative populations of the composition of neutron stars. Our calculation indicates that, when the kaon optical potential is deep enough, for instance, $-U_K > 127$ and 115 MeV for parameter sets GM1 and GM3, respectively, the Ξ^- hyperon does not appear in the matter. The result obtained for parameter set GM3 in this case is illustrated in Fig. 6, and that for parameter set GM1 in Fig. 7. The main feature shown in these figures is that the onset density of K^- condensation is shifted to a higher value with the inclusion of the δ-meson channel interaction compared to that lacking it. To understand why inclusion of the δ-meson channel interaction shifts the onset density of kaon condensation to a higher one, we implement the characteristics of kaon-kaon interactions

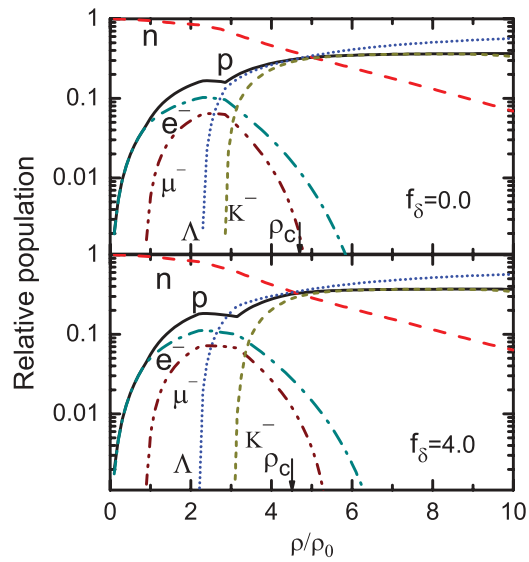

FIG. 7. (Color online) The same as Fig. 6 but using parameter set GM1 and $U_K = -130$ MeV.

provided by exchanging the isovector mesons ρ and δ. It is known that the δ-meson channel interaction is attractive but the ρ-meson channel is repulsive. When the δ-meson channel interaction plays the main role, this favors the onset of kaons at a lower density. In contrast, when the ρ-meson channel interaction plays the main role, this favors the onset of kaons at a higher density. In the parameter fitting, we maintain the bulk properties of nuclear matter, the effective nucleon mass, and the compression modulus the same in the two cases with and without the δ-meson channel interaction. With the fitted parameters reported in Table I, we can see that the coupling parameter f_ρ is greatly enhanced with consideration of the δ-meson channel interaction. The coupling parameter $g_{\rho K}$ is thus also enhanced owing to the relation $g_{\rho K} = g_{\rho N}$ from the SU(6) quark model. So the repulsive channel interaction is strengthened. As a consequence, the onset density for kaon condensation to appear is shifted to a higher one as the δ-meson channel interaction is taken into account. Moreover, to examine the effect of $x_{\delta K}$, we perform a series of calculations with various values of $x_{\delta K}$ in parameter set GM1 and $U_K = -160$ MeV. We find that the onset density becomes higher when the value of $x_{\delta K}$ increases. However, no solution was found in the calculation, as $x_{\delta K}$ is larger than 0.3. Because the presence of K^- condensation will exert an important influence on the properties of neutron stars by softening the EOS, the delayed onset of K^- condensation will give rise to some results differing from those without the δ-meson channel interaction, which is shown later in detail. In addition, the disappearances of charged leptons e^- and μ^- are also shifted to higher densities to maintain the charge neutrality of the system.

With the Gibbs criteria, when kaons first appear in the interior of a neutron star, the kaon condensation phase, which is composed of kaons, baryons, and leptons, occupies only part of the whole volume of the system, and the other part is still in the normal (baryon) phase, which is composed of baryons and leptons. The two phases coexist with the same pressure. Because of the difference in the compositions, baryons are allowed to have different effective masses in the two phases.

To show the properties of kaonic neutron star matter and the structure of the stars clearly, we illustrate the calculated results of the effective masses of baryons in the matter with parameter set GM3 in Fig. 8 and those with parameter set GM1 in Fig. 9. These figures show that with an increase in baryon density, the configurations in the interior of the neutron star can be divided into three parts: (I) the pure normal phase; (II) the mixed phase (with both normal phase and kaon condensation phase); and (III) the pure kaon condensation phase. The pure normal phase exists in a relatively lower density range. Then the mixed phase emerges. With an increase in density, the mixed phase will disappear. Then only the pure kaon condensation phase is left behind at a very high density. In the case without the δ-meson channel interaction, the neutron and proton are isospin degenerate with the same effective mass, as shown in the upper panels in Figs. 8 and 9. However, in the case with the δ-meson channel interaction, the effective masses of the neutron and proton split, and the difference between them at a higher density decreases after reaching a maximum value (which can be as large as about 100 MeV). This implies the restoration of isospin symmetry of the nuclear force at high densities. Comparing Figs. 8 and 9,

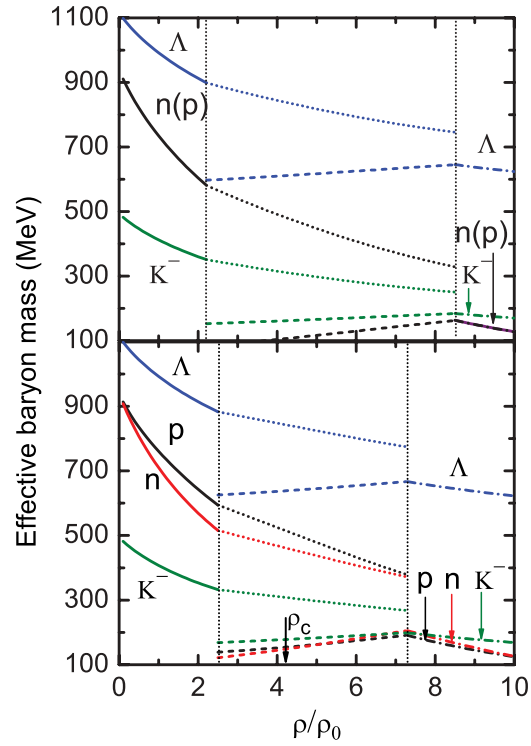

FIG. 8. (Color online) Calculated variation behaviors of the effective masses of the baryons and the kaon with respect to baryon density in the case of parameter set GM3 with kaon potential $U_K = -130$ MeV. The upper panel is the result without the δ-meson channel interaction, and the lower panel is that with the δ-meson channel interaction.

one notices that the density range for the existence of the mixed phase obviously depends on the parameter set, and the coexisting range for parameter set GM1 is much narrower than that for GM3. The δ-meson channel interaction also reduces the density range of the mixed phase. Moreover, a distinct characteristic of the mixed phase is that a new solution of the effective baryon mass that coincides with that in the pure kaon condensation phase appears, in addition to the one connecting with that in the normal phase. More specifically, in the mixed phase, the effective mass of each species of baryon in the normal phase is much larger than that in the kaon phase. And the effective baryon masses connecting with those in the pure kaon phase increase with increasing baryon density. These features may be referred to a direct manifestation of different dynamics between the normal phase and the kaon phase. The effective mass of the kaon is also included in Figs. 8 and 9. With inclusion of the δ-meson channel interaction, the effective mass of kaons is relatively smaller than that without the δ mesons in the normal phase and the pure kaon phase, however, it is slightly larger than that in the case without the δ mesons in the mixed phase. In addition, by comparing the critical density at which the mixed phase disappears and the central density of the neutron star obtained by solving the TOV equation, we find that the pure kaon phase can be realized in the core of a neutron star with parameter set GM1, but it does not appear with parameter set GM3 when the δ-meson channel interaction is included.

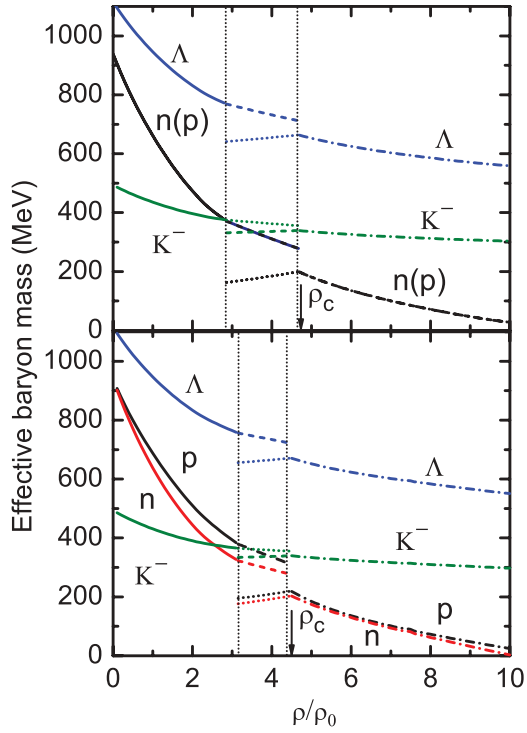

FIG. 9. (Color online) The same as Fig. 8 but using parameter set GM1 and $U_K = -130$ MeV.

To demonstrate the effect of the kaon optical potential, we demonstrate the EOSs of kaonic neutron star matter calculated with parameter set GM3 and several kaon optical potentials in Fig. 10 and those obtained with parameter set GM1 in Fig. 11. Clearly, the onset of kaon condensation is highly dependent on the kaon optical potential, which has not yet been well determined by experiment. Specifically, the smaller the absolute value of U_K, the higher the onset baryon (energy) density of kaon condensation. However, the effect of the δ-meson channel interaction shrinking the range of the mixed phase is general; it does not depend on the strength of the

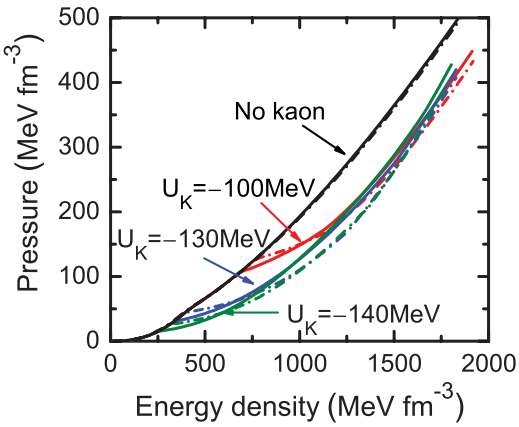

FIG. 10. (Color online) Calculated equations of state of neutron star matter with kaon condensation using parameter set GM3 with different kaon optical potentials. Solid curves are the results without the δ-meson channel interaction, and the dash-dotted curves are those with the δ-meson channel interaction.

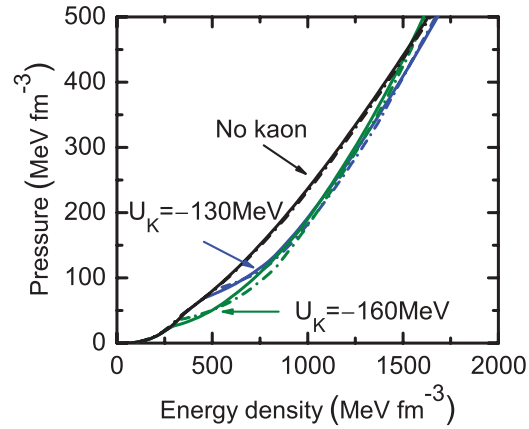

FIG. 11. (Color online) The same as Fig. 10 but for parameter set GM1.

kaon optical potential U_K. For the same U_K, the appearance of K^- condensation with the inclusion of the δ-meson channel interaction is shifted to a higher energy density, corresponding to a higher baryon density, as illustrated in Figs. 6 and 7. Comparing Fig. 3 with Figs. 10 and 11, one can see that, for a neutron star with kaon condensation, the EOS of neutron star matter with the δ-meson channel interaction remains stiffer than that without the δ-meson channel interaction over a larger energy density range than that in the case when only hyperons are considered. The reason for this phenomenon is that inclusion of the δ-meson channel interaction delays the onset of kaon condensation to a higher density. Nevertheless, for parameter set GM3, the EOS with antikaons and without the δ mesons becomes stiffer than that with the δ-mesons in the high-density region.

With the EOSs of neutron star matter with kaon condensation, we obtain the mass-radius relations of the stars by solving the TOV equation. The results for parameter set GM3 are illustrated in Fig. 12, and those for GM1 in Fig. 13. The results obtained for the properties of neutron stars with

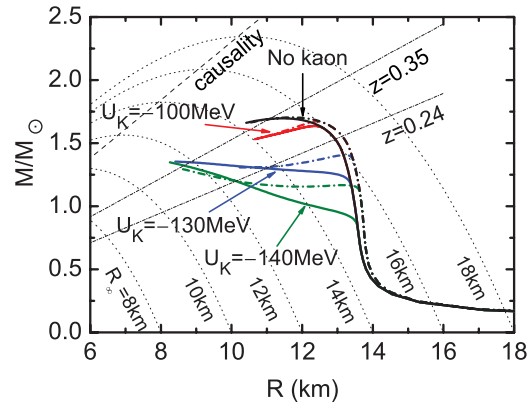

FIG. 12. (Color online) Observation constraints on mass-radius relations of neutron stars calculated with parameter set GM3 and several kaon optical potentials (the ones marked with either "No kaon" or "$U_K = -100$ MeV" are for those composed of the matter preassigned not including Ξ^- hyperons). Solid curves are the results without the δ-meson channel interaction, and dash-dotted curves are those with the δ-meson channel interaction.

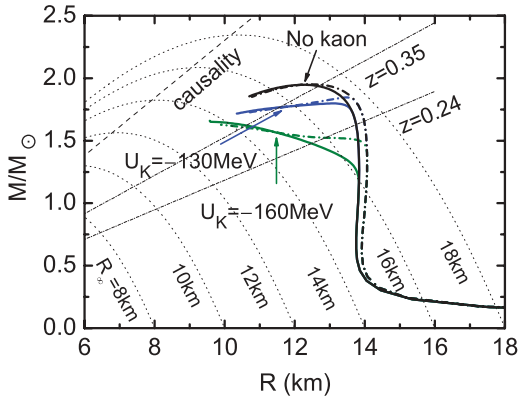

FIG. 13. (Color online) The same as Fig. 12 but for parameter set GM1.

maximum masses, the corresponding onset density of the mixed phase, and that of the pure kaon phase for different parameter sets are listed in Table III. In this table, one can note that, for parameter set GM3, the pure kaonic phase cannot appear in the maximum-mass kaonic neutron stars if the kaon optical potential is not very strong, for example, in the case of $U_K = -100$ MeV, or even $U_K = -130$ MeV, with inclusion of the δ-meson channel interaction.

Comparing the data listed in Tables II and III and looking over the mass-radius relations shown in Fig. 12, we find that the appearance of kaon condensation reduces the maximum mass and accelerates the instability of the neutron star if the kaon optical potential is neither very weak nor very strong. For instance, in the case of $U_K = -100$ MeV, kaon condensation enhances the instability of the star obviously. According to this phenomenon, it was once claimed that the appearance of kaon condensation will lead to the formation of black holes [53]. However, such a result depends on the model parameters, especially on the kaon optical potential U_K. The critical values of U_K are -126 MeV in the case without the δ-meson channel interaction and -143 MeV with the δ-meson channel interaction for parameter set GM3, and they are -144 and -152 MeV, respectively, for the cases without and with the δ-meson channel interaction for GM1. The critical values of U_K will be much larger for the case without hyperons. If the kaon optical potential U_K is stronger than the critical one for each parameter set, a neutron star can be stable even with the appearance of kaon condensation. For instance, a stable neutron star series can be realized with kaon optical potential $U_K = -140$ MeV as displayed in Fig. 12. For this case, it is remarkable that, in the radius range of about $R = 11$–13.5 km, the mass of a kaonic neutron star with the δ-meson channel interaction is larger than that without the interaction, but the result reverses for the stars with smaller radii. The reason is that the EOS with the δ-meson channel interaction is stiffer (softer) at low (high) densities than that without the δ-meson channel interaction. This is similar to the discussion of hyperonic neutron stars in Sec. III A. A similar result was also obtained for hybrid neutron stars with hyperons and a quark core [69].

In Fig. 12, one can also note that, in the case of parameter set GM3, the maximum mass of stable neutron stars with kaon condensation is less than the canonical Hulse-Taylor pulsar B1931 + 16, with a mass of $1.44 M_\odot$ [95]. Thus, this set of parameters may be ruled out. In another case, looking at Fig. 13, one can recognize that, with parameter set GM1, the maximum mass for a stable neutron star can be enhanced to $1.66 M_\odot$ with $U_K = -160$ MeV, compatible with the observation at a reasonable confidence level. Furthermore, our calculation shows that, for neutron stars whose hadron composition does not include kaon condensation, the radius cannot be smaller than 12 km, but for neutron stars with both hyperons and antikaon condensation, the radius can be even less than 10 km. If the radius of a neutron star is identified as being smaller than 12 km, one can conclude that a kaonic neutron star with hyperons is favored. Identification of the existence of exotic matter in a compact star requires at least several precise observations of the neutron star's radius and mass simultaneously. Unfortunately, the present single-neutron star observation cannot give such a precise result. However, other observations from gravitational red shift and X-ray burst in X-ray binaries can provide some useful information, which is discussed in Sec. III C.

From the mass-radius relations, it seems that for some parameter sets, for example, GM1 with $U_K = -130$ MeV, a star will become unstable as soon as K^- mesons appear, but from Fig. 9 one can see that the pure kaon phase can be realized. In fact, in this case the onset of K^- does not result in instability of the star immediately. Instability of the star occurs when the richness of K^- has increased greatly. This scenario is not easily identified from the mass-radius relation. However, it can be clearly seen from the relation between a neutron star's mass and its central density. We thus display the calculated corresponding functions of a neutron star family

TABLE III. Calculated results of the properties of neutron stars with maximum masses for several sets of parameters (the ones in GM3 with $U_K = -100$ MeV are for those composed of the matter preassigned not including Ξ^- hyperons). Here $\rho_{\rm mix}$ and ρ_{pk} represent the onset density of the mixed phase and the pure kaonic phase, respectively. ρ_c represents the central density.

	GM3	GM3(δ)	GM3	GM3(δ)	GM3	GM3(δ)	GM1	GM1(δ)	GM1	GM1(δ)
U_K (MeV)	-100	-100	-130	-130	-140	-140	-130	-130	-160	-160
$M_{\rm max}$ ($M_\odot$)	1.64	1.67	1.35	1.41	1.35	1.30	1.78	1.81	1.66	1.63
R (km)	12.35	12.43	8.41	13.21	8.25	8.55	13.11	13.49	9.58	9.89
ρ_c/ρ_0	5.5	5.7	12.9	4.2	11.8	11.5	4.8	4.5	9.4	8.9
$\rho_{\rm mix}/\rho_0$	4.1	4.6	2.2	2.5	1.7	2.0	2.8	3.1	1.9	2.1
ρ_{pk}/ρ_0	–	–	8.5	–	9.3	7.8	4.7	4.4	5.6	5.0

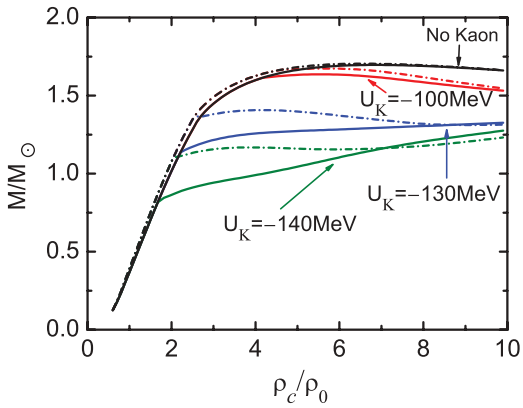

FIG. 14. (Color online) Calculated results of the mass of a neutron star as a function of the central density using parameter set GM3 and several kaon optical potentials. Solid curves are results without the δ-meson channel interaction, and dash-dotted curves are those with the δ-meson channel interaction.

with parameter set GM3 in Fig. 14 and that with parameter set GM1 in Fig. 15. These figures show that for $U_K = -130$ MeV, neutron stars are still stable after the appearance of K^-. They become unstable until their masses begin to decrease with increasing central density.

Recalling both the results of prior studies and our discussion in Sec. III A, one knows that, when only the baryon octet is considered, Ξ^- hyperons can appear at a certain density denoted ρ_a here. And if the onset density of Ξ^- is lower than that of K^-, the appearance of Ξ^- hyperons shifts the onset density of kaon condensation to a higher one [48]. Thus Ξ^- hyperons may influence the properties of a kaonic neutron star greatly. However, in the preceding discussion, we did not pay attention to the effect of Ξ^- hyperons. The reasons for this are as follows. First, as already mentioned, if the kaon optical potential is deep enough (the corresponding critical values are $|U_K| = 127$ and 115 MeV for parameter sets GM1 and GM3, respectively), the onset density of K^- is lower than the ρ_a defined here; in fact, Ξ^- hyperons do not appear in the matter preassigned to include both hyperons and kaons. To demonstrate this feature better, we take the underlying characteristic into account. Our calculation shows that, in this case, the chemical potential of Ξ^- hyperons, μ_{Ξ^-}, is less than the mass m_{Ξ^-} in the medium with the appearance of K^-. Therefore Ξ^- hyperons do not appear in the case where the kaon optical potential is strong enough. Second, if the kaon optical potential is very shallow, K^- mesons emerge at a relatively higher density, and Ξ^- hyperons may appear before the onset of K^-. In our practical calculation, we only encounter this case with $U_K > -115$ MeV (e.g., $U_K = -100$ MeV) in parameter set GM3. In this case, the appearance of Ξ^- hyperons delays the onset of K^- to a higher density, and the δ-meson channel interaction reinforces this scenario, as it lowers the onset density of Ξ^-. However, for this case, just as Ref. [48] has shown, Ξ^- hyperons as fermions are restricted by the Pauli principle, and K^- mesons as bosons can form Boson-Einstein condensation. These characters lead to the appearance of K^- quenching all particles with a negative electric charge. Moreover, the mass-radius relation curve given by this parameter set is quite far away from the critical, stable one, so the aforementioned result regarding the relation of the critical optical potential to the stability of the kaonic neutron star is not influenced by the appearance of Ξ^- hyperons with a shallow optical potential.

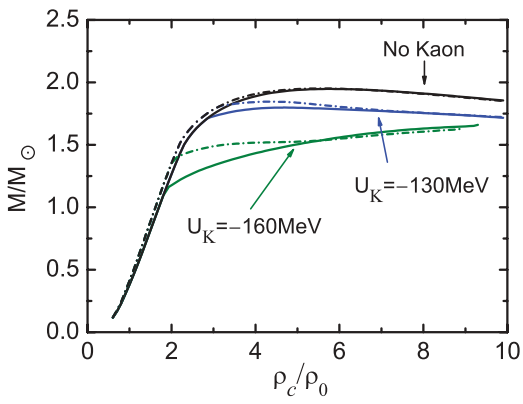

FIG. 15. (Color online) The same as Fig. 14 but for parameter set GM1.

C. Observation constraints on neutron stars including kaon condensation

To investigate the inner composition and structure of neutron stars, we must compare the calculated results with astronomical observations. In the following, we present some possible constraints on the neutron stars with kaon condensation from neutron star observations.

According to Brown's scenario, the K^- meson plays a very important role in the evolving process of neutron stars in the neutron star binary. The accepted scenario of the evolution of the neutron star binary is that, when a companion giant evolves, the giant and the first-born neutron star go into a common envelope, so that accretion onto the first-born neutron star is limited by the Eddington rate and is negligible. However, after Chevalier's suggestion [96], Ref. [52] showed that the rate of accretion required may go over to hypercritical accretion and could be sufficient to send the first-born neutron star into a black hole. Furthermore, Brown *et al.* [52,54] proposed an alternative scenario of binary neutron star evolution. According to Brown's scenario, the two giant progenitors of neutron stars in a binary must burn helium at the same time and the generated neutron stars in the binary have to be within 4% of each other in mass; otherwise, the first-born neutron star will accrete matter from its companion in the red giant phase and then go into a black hole with the onset of antikaon condensation. This scenario for binary neutron stars also predicts that there are about 5 times more low-mass black hole/neutron star binaries than neutron star/neutron star binaries. It is easy to rule out this prediction if one can find an accurately measured neutron star/nuclear star binary in which the neutron stars are more than 4% different from each other in mass. However, to date, with well-observed neutron star binaries, this scenario works quite well (details are given in Refs. [2] and [54]).

One of the conclusions in Brown's scenario is that the onset of antikaon condensation will lead to the neutron

star collapsing into a black hole. We compare the preceding calculated results and Brown's scenario with some neutron star observations. The first thing we emphasize is the reduction in the mass of pulsar J0751 + 1807 with the reported $(2.1 \pm 0.2)M_\odot$ [97] to $(1.26 \pm 0.14)M_\odot$ [98]. This reduction alleviates considerably the dispute that the appearances of hyperons, kaon condensation, and quarks soften, in principle, the EOS and thus produce a relatively smaller maximum neutron-star mass, but the observation gives a highly massive star.

The gravitational red shift z is a very useful quantity for observations [2]; it has a simple relation with the mass and radius of a neutron star:

$$z = \left(1 - \frac{2GM}{Rc^2}\right)^{-1/2} - 1. \tag{31}$$

The best measurement of z was once claimed to be that of EXO 0748-676 with X-ray bursts [2]. The spectrum analysis showed that there exist two resonance scattering lines that are consistent with Fe XXV and XXVI spectra for $z = 0.35$ [99]. If the spectral identification is correct, it can be used to constrain the mass-radius relations given by different model parameters. Therefore, we illustrate the contour with the red shift $z = 0.35$ in Figs. 12 and 13. Obviously, for parameter set GM3, only the case with $U_K = -100$ MeV does not cross the curve given by $z = 0.35$, and other cases with kaon condensation lead to a maximum mass of neutron stars less than that of the Hulse-Taylor pulsar [95]. For parameter set GM1, all three cases cross the observation curve, but the case with $U_K = -130$ MeV cannot in fact be realized because the neutron star obtained is unstable in this case. This indicates that only the neutron stars composed of the matter not including antikaon condensation and the stable ones with antikaon condensation may exist with parameter set GM1. What is more, it should be noted that $z = 0.24$ has been identified with different simulation codes for the same observation data by the Fe XXIV absorption feature [100], and the mass of neutron star EXO 0748-676 is reduced to $M \geqslant 1.48M_\odot$ with such a red shift [100,101]. This result is more consistent with a detailed multiwavelength analysis showing that the mass of a compact star is more compatible with $M \geqslant 1.35M_\odot$ [102]. If the red shift $z = 0.24$ is well accepted, the constraint on the model parameters will be weakened apparently, as shown in Figs. 12 and 13.

Another useful quantity for observations is the thermal radiation radius

$$R_\infty = R/\sqrt{1 - 2GM/Rc^2}, \tag{32}$$

coming from thermal observations of a neutron star's surface. Most known neutron stars observed as pulsars emit photons dominated by nonthermal emissions. Such emissions are generated in a neutron star's magnetosphere and are difficult to apply to limit the macroscopic properties of neutron stars. However, constraints on the neutron star radius can be obtained by fitting the spectrum of the X-ray emission if the temperature, the composition of the atmosphere, and the distance are known and the surface magnetic field is very weak. These conditions are fulfilled by quiescent low-mass X-ray binaries (qLMXBs), especially those in globular clusters [103,104]. With the assumption that the total photon fluxes at the surface of a neutron star are those of a blackbody, they should obey the relation

$$F_\infty = L_\infty/4\pi d^2 = \sigma T_\infty^4 (R_\infty/d)^2, \tag{33}$$

where d is the distance and F_∞, L_∞, and T_∞ are the flux, luminosity, and temperature, respectively. With the relations $T_\infty = T/(1+z)$ and $F_\infty = F/(1+z)^2$, R_∞ can be determined if F_∞ and T_∞ are well measured. With the R_∞ obtained, we can constrain the mass-radius relation of the neutron star. We thus illustrate the contours relevant to several values of R_∞ in Figs. 12 and 13.

As for observations, two sources in cluster Omega Cen show $R_\infty = 14.3 \pm 2.1$ km [104] and $R_\infty = 13.6 \pm 0.3$ km [105], respectively. However, some fits were carried out by implementing a fixed surface gravity $\log g_s = 14.383$. In fact, a wide range of g_s needs to be taken into account in self-consistent spectral fitting for the possible neutron star mass and radius. With such a consideration of the whole range of fitted g_s, Heinke *et al.* obtained $R_\infty \simeq 16$–20 km for qLMXB X7 in the globular cluster 47 Tuc [106]. However, in these calculations, all the fits are performed with hydrogen atmosphere, a possible drawback, as pointed out in Refs. [103,107] is that it is not yet possible to exclude the case that the accretion is still going on at very low rate, and adding constantly to the atmosphere heavy elements that will affect the spectral identification.

Considering the uncertainties in the simulation and observation, and combining other constraints, one can recognize that the case for parameter set GM1 and with optical potential $U_K = -160$ MeV is the one most possible to exist practically. For other cases, owing to the instability shown in Fig. 13, the neutron star will spontaneously adjust its chemical composition through weak and/or strong interaction(s) to resist the great pressure and may go into a black hole if it can accrete enough matter from its surroundings, just as described by Brown's scenario. As we pointed out in Sec. III B, if the kaon optical potential U_K is less than -144 MeV (-152 MeV with the δ meson) for parameter set GM1, neutron stars will be stable with the onset of kaon condensation. From this we can see that the kaon optical potential plays a highly significant role in determining the stability of neutron stars and it is related to their compositions. Meanwhile, concerning kaon condensation, we find that parameter set GM1 is favored by observations.

Finally, compared with neutron stars composed of matter including kaon condensation but no hyperons, neutron stars with both kaon condensation and hyperons have a relatively lower critical density for the appearance of kaon condensation and the corresponding maximum mass and central density of the stars are also slightly lowered. However, it is still difficult to distinguish the two cases from observations at present, because there are several uncertain parameters, such as the kaon optical potential, the effective nucleon mass, and the compression modulus. If some of these parameters are fixed exactly by nuclear experiments, it is possible to distinguish the two cases. In contrast, if several masses and radii of neutron stars can be determined precisely, this also provides the chance to distinguish the two cases. However, from the theoretical point of view, if we consider antikaons composed of strange quarks in the interior of a neutron star, it is better to include hyperons in the consideration of β equilibrium.

IV. SUMMARY

In this paper, we have investigated in detail the influence of the isovector-scalar (δ-meson) channel interaction on the properties of neutron stars with the presence of both hyperons and kaon condensation in the framework of the RMF approach. Generally, for the simplest neutron star, whose baryon composition includes only protons and neutrons, without antikaon condensation, the δ-meson channel interaction stiffens the EOS when the energy density is lower than 950 MeV fm^{-3} and then softens it with increasing energy density. However, once hyperons are taken into account, the δ-meson channel interaction only stiffens the EOS before the onset of hyperons, that is, at lower energy densities, less than about 500 MeV fm^{-3}, and softens the EOS of matter that consists of not only nucleons but also hyperons. A similar result is obtained for neutron stars with kaon condensation. It is also remarkable that the δ-meson channel interaction shifts the presence of K^- condensation to a higher baryon density, which may make a significant change in the macroscopic properties of neutron stars because the EOS is softened when K^- mesons appear.

We have also discussed the mass-radius relations of neutron stars in cases with and without the δ-meson channel interaction. In the case of neutron stars with only hyperons, for each parameter set of the RMF, the difference in maximum masses obtained between those with and those without the δ-meson channel interaction is very small, but for neutron stars with the same mass, the radius of neutron stars with the δ-meson channel interaction is much larger than that of stars without the δ-meson channel interaction. As for neutron stars including both hyperons and kaon condensation, neutron star masses with the δ-meson interaction are larger than those without the δ-meson interaction at larger radii, but the results are reversed for those with smaller radii.

Furthermore, we have studied the stability of neutron stars with hyperons and antikaons and found that the stability is highly dependent on the kaon optical potential. The critical values of the kaon potential U_K are -144 MeV without the δ-meson channel interaction and -152 MeV with the inclusion of the δ mesons in the case of parameter set GM1, and they are -126 MeV and -143 MeV, respectively, for the cases without and with the δ-meson channel interaction for GM3. If U_K is smaller than the respective critical value for each parameter set, stable neutron stars with antikaon condensation can be obtained.

Finally, we have compared the calculated results with astrophysical observations and given some possible constraints on the model parameters. The theoretical calculation shows that for neutron stars with only the baryon octet, the radius cannot be smaller than 12 km, but for those with both hyperons and antikaon condensation, the minimum radius can be even less than 10 km. If the radius of a neutron star can be identified to be smaller than 12 km in observations, a kaonic neutron star will be favored. Identification of the existence of exotic matter in a compact star requires at least several precise observations of the neutron star's radius and mass simultaneously. Although the present observation of a single neutron star cannot give such a precise result, observations from gravitational red shift and X-ray burst in X-ray binaries provides some useful information, and the combination of these observations shows that neutron stars with both hyperons and antikaon condensation are more favored than neutron stars with only hyperons, although some uncertainties in the observations still exist. The observations also show that the model parameter set with a larger compression module and smaller nucleon mass at saturation density (e.g., GM1) is favored.

ACKNOWLEDGMENTS

This work was supported by the National Natural Science Foundation of China under Contract Nos. 10425521 and 10935001 and the Major State Basic Research Development Program under Contract No. G2007CB815000.

[1] J. Lattimer and M. Prakash, Science **304**, 536 (2004).
[2] J. Lattimer and M. Prakash, Phys. Rep. **442**, 109 (2007).
[3] N. K. Glendenning, Astrophys. J. **293**, 470 (1985).
[4] F. Weber and M. K. Weigel, Nucl. Phys. A **493**, 549 (1989); **505**, 779 (1989).
[5] M. Rufa, J. Schaffner, J. Maruhn, H. Stocker, W. Greiner, and P. G. Reinhard, Phys. Rev. C **42**, 2469 (1990).
[6] S. K. Ghosh, S. C. Phatak, and P. K. Saha, Z. Phys. A **352**, 457 (1995).
[7] J. Schaffner and I. N. Mishustin, Phys. Rev. C **53**, 1416 (1996).
[8] I. Bednarek and R. Manka, J. Phys. G **31**, 1009 (2005).
[9] J. Schaffner-Bielich, Nucl. Phys. A **804**, 309 (2008).
[10] Z. G. Dai and K. S. Cheng, Phys. Lett. B **401**, 219 (1997).
[11] N. K. Glendenning and J. Schaffner-Bielich, Phys. Rev. Lett. **81**, 4564 (1998); Phys. Rev. C **60**, 025803 (1999).
[12] S. Banik and D. Bandyopadhyay, Phys. Rev. C **64**, 055805 (2001).
[13] H. Guo, Y. Chen, B. Liu, Q. Zhao, and Y. Liu, Phys. Rev. C **68**, 035803 (2003).
[14] J. F. Gu, H. Guo, R. Zhou, B. Liu, X. G. Li, and Y. X. Liu, Astrophys. J. **622**, 549 (2005).
[15] D. P. Menezes, P. K. Panda, and C. Providência, Phys. Rev. C **72**, 035802 (2005).
[16] T. Maruyama, T. Muto, T. Tatsumi, K. Tsushima, and A. W. Thomas, Nucl. Phys. A **760**, 319 (2005).
[17] G. E. Brown, C. H. Lee, H. J. Park, and M. Rho, Phys. Rev. Lett. **96**, 062303 (2006).
[18] T. Maruyama, T. Tatsumi, D. N. Voskresensky, T. Tanigawa, T. Endo, and S. Chiba, Phys. Rev. C **73**, 035802 (2006).
[19] A. Li, G. F. Burgio, U. Lombardo, and W. Zuo, Phys. Rev. C **74**, 055801 (2006).
[20] A. Mishra and S. Schramm, Phys. Rev. C **74**, 064904 (2006).
[21] J. O. Andersen, Phys. Rev. D **75**, 065011 (2007).
[22] C. Y. Ryu, C. H. Hyun, S. W. Hong, and B. T. Kim, Phys. Rev. C **75**, 055804 (2007).
[23] G. H. Wang, W. J. Fu, and Y. X. Liu, Phys. Rev. C **76**, 065802 (2007).

[24] G. H. Wang, W. J. Fu, and Y. X. Liu, Phys. Rev. C **78**, 025801 (2008).
[25] T. Muto, Nucl. Phys. A **754**, 350c (2005); Phys. Rev. C **77**, 015810 (2008).
[26] F. Weber and M. K. Weigel, Nucl. Phys. A **505**, 779 (1989).
[27] H. Huber, F. Weber, M. K. Weigel, and Ch. Schaab, Int. J. Mod. Phys. E **7**, 301 (1998).
[28] X. Hu and H. Guo, Phys. Rev. C **67**, 038801 (2003).
[29] Y. J. Chen, H. Guo, and Y. X. Liu, Phys. Rev. C **75**, 035806 (2007); Y. J. Chen, Y. F. Yuan, and Y. X. Liu, *ibid.* **79**, 055802 (2009).
[30] N. K. Glendenning, Phys. Rev. D **46**, 1274 (1992); N. K. Glendenning and F. Weber, Astrophys. J. **400**, 647 (1992); N. K. Glendenning, Phys. Rep. **264**, 143 (1996).
[31] D. B. Blaschke, H. Grigorian, G. Poghosyan, C. D. Roberts, and S. Schmidt, Phys. Lett. B **450**, 207 (1999).
[32] E. S. Fraga, R. D. Pisarski, and J. Schaffner-Bielich, Phys. Rev. D **63**, 121702(R) (2001).
[33] Y. X. Liu, D. F. Gao, and H. Guo, Nucl. Phys. A **695**, 353 (2001); Y. X. Liu, D. F. Gao, J. H. Zhou, and H. Guo, *ibid.* **725**, 127 (2003); L. Chang, Y. X. Liu, and H. Guo, *ibid.* **750**, 324 (2005); J. F. Gu, H. Guo, X. G. Li, Y. X. Liu, and F. R. Xu, Phys. Rev. C **73**, 055803 (2006); Eur. Phys. J. A **30**, 455 (2006).
[34] R. X. Xu, Astrophys. J. **570**, L65 (2002); **596**, L59 (2003).
[35] S. B. Ruster and D. H. Rischke, Phys. Rev. D **69**, 045011 (2004).
[36] N. Prasad and R. S. Bhalerao, Phys. Rev. D **69**, 103001 (2004).
[37] F. Weber, Prog. Part. Nucl. Phys. **54**, 193 (2005).
[38] M. Alford, M. Braby, M. Paris, and S. Reddy, Astrophys. J. **629**, 969 (2005); M. Alford, D. B. Blaschke, A. Drago, T. Klähn, G. Pagliara, and J. Shaffner-Bielich, Nature **445**, E7 (2007).
[39] A. K. Sisodiya, R. S. Kaushal, D. Parashar, and V. S. Bhasin, J. Phys. G **34**, 929 (2007).
[40] F. Yang and H. Shen, Phys. Rev. C **77**, 025801 (2008).
[41] D. B. Kaplan and A. E. Nelson, Phys. Lett. B **175**, 57 (1986); **179**, 409 (1986).
[42] G. E. Brown, K. Kubodera, M. Rho, and V. Thorsson, Phys. Lett. B **291**, 355 (1992); C. H. Lee, G. E. Brown, and M. Rho, *ibid.* **335**, 266 (1994).
[43] V. Thorsson, M. Prakash, and J. M. Lattimer, Nucl. Phys. A **572**, 693 (1994).
[44] P. J. Ellis, R. Knorren, and M. Prakash, Phys. Lett. B **349**, 11 (1995).
[45] R. Knorren, M. Prakash, and P. J. Ellis, Phys. Rev. C **52**, 3470 (1995).
[46] M. Prakash, I. Bombaci, M. Prakash, P. J. Ellis, J. M. Lattimer, and R. Knorren, Phys. Rep. **280**, 1 (1997).
[47] P. Yue and H. Shen, Phys. Rev. C **77**, 045804 (2008).
[48] S. Banik and D. Bandyopadhyay, Phys. Rev. C **66**, 065801 (2002).
[49] H. Guo, B. Liu, and J. Zhang, Phys. Rev. C **67**, 024902 (2003).
[50] R. C. Tolman, Phys. Rev. **55**, 364 (1939).
[51] J. R. Oppenheimer and G. M. Volkoff, Phys. Rev. **55**, 374 (1939).
[52] G. E. Brown and H. A. Bethe, Astrophys. J. **423**, 659 (1994).
[53] G. E. Brown, Astrophys. J. **440**, 270 (1995).
[54] G. E. Brown, C. H. Lee, and M. Rho, Phys. Rep. **462**, 1 (2008).
[55] J. A. Pons, Juan A. Miralles, M. Prakash, and J. M. Lattimer, Astrophys. J. **553**, 382 (2001).
[56] J. D. Walecka, Ann. Phys. **83**, 491 (1974); B. D. Serot and J. D. Walecka, in *Advances in Nuclear Physics*, edited by J. W. Negele and E. Vogt (Plenum Press, New York, 1986), Vol. 16, p. 1; B. D. Serot and J. D. Walecka, Int. J. Mod. Phys. E **6**, 515 (1997); P. G. Reinhard, Rep. Prog. Phys. **52**, 439 (1989); P. Ring, Prog. Part. Nucl. Phys. **37**, 193 (1996); M. Bender, P.-H. Heenen, and P. G. Reinhard, Rev. Mod. Phys. **75**, 121 (2003); J. Meng, H. Toki, S. G. Zhou, S. Q. Zhang, W. H. Long, and L. S. Geng, Prog. Part. Nucl. Phys. **57**, 470 (2006).
[57] N. K. Glendenning, *Compact Stars* (Springer-Verlag, Berlin, 2000).
[58] J. Boguta and A. R. Bodmer, Nucl. Phys. A **292**, 413 (1977).
[59] Y. Sugahara and H. Toki, Nucl. Phys. A **579**, 557 (1994).
[60] H. Müller and B. D. Serot, Nucl. Phys. A **606**, 508 (1996).
[61] C. J. Horowitz and J. Piekarewicz, Phys. Rev. Lett. **86**, 5647 (2001); Phys. Rev. C **64**, 062802(R) (2001)
[62] J. K. Bunta and S. Gmuca, Phys. Rev. C **68**, 054318 (2003); **70**, 054309 (2004).
[63] B. G. Todd-Rutel and J. Piekarewicz, Phys. Rev. Lett. **95**, 122501 (2005).
[64] M. M. Haidari and M. M. Sharma, Nucl. Phys. A **803**, 159 (2008).
[65] G. Y. Shao and Y. X. Liu, Phys. Rev. C **79**, 025804 (2009).
[66] S. Kubis and M. Kutschera, Phys. Lett. B **399**, 191 (1997).
[67] B. Liu, V. Greco, V. Baran, M. Colonna, and M. Di Toro, Phys. Rev. C **65**, 045201 (2002); B. Liu, M. Di Toro, V. Greco, C. W. Shen, E. G. Zhao, and B. X. Sun, *ibid.* **75**, 048801 (2007).
[68] A. Sulaksono, P. T. P. Hutauruk, and T. Mart, Phys. Rev. C **72**, 065801 (2005).
[69] D. P. Menezes, and C. Providência, Phys. Rev. C **70**, 058801 (2004).
[70] A. W. Steiner, M. Prakash, J. M. Lattimer, and P. J. Ellis, Phys. Rep. **411**, 325 (2005).
[71] M. Di Toro *et al.*, Prog. Part. Nucl. Phys. **62**, 389 (2008).
[72] B. A. Li, L. W. Chen, and C. M. Ko, Phys. Rep. **464**, 113 (2008).
[73] M. L. Cescato and P. Ring, Phys. Rev. C **57**, 134 (1998).
[74] N. K. Glendenning and S. A. Moszkowski, Phys. Rev. Lett. **67**, 2414 (1991).
[75] J. Zimanyi and S. A. Moszkowski, Phys. Rev. C **42**, 1416 (1990).
[76] N. K. Glendenning, F. Weber, and S. A. Moszkowski, Phys. Rev. C **45**, 844 (1992).
[77] N. K. Glendenning, Phys. Lett. B **114**, 392 (1982); Astrophys. J. **293**, 470 (1985); Z. Phys. A **326**, 57 (1987).
[78] R. Machleidt, Adv. Nucl. Phys. **19**, 189 (1989).
[79] J. Schaffner, C. B. Dover, A. Gal, C. Greiner, and H. Stöcker, Phys. Rev. Lett. **71**, 1328 (1993).
[80] D. J. Millener, C. B. Dover, and A. Gal, Phys. Rev. C **38**, 2700 (1988).
[81] J. Schaffner, C. B. Dover, A. Gal, D. J. Millener, C. Greiner, and H. Stöcker, Ann. Phys. (NY) **235**, 35 (1994).
[82] S. Bart *et al.*, Phys. Rev. Lett. **83**, 5238 (1999).
[83] H. Noumi *et al.*, Phys. Rev. Lett. **89**, 072301 (2002); P. K. Saha *et al.*, Phys. Rev. C **70**, 044613 (2004).
[84] C. J. Batty, E. Friedman, and A. Gal, Phys. Lett. B **335**, 273 (1994); Prog. Theor. Phys. Suppl. **117**, 227 (1994).
[85] J. Mareš, E. Friedman, A. Gal, and B. K. Jennings, Nucl. Phys. A **594**, 311 (1995).
[86] E. Friedman and A. Gal, Phys. Rep. **452**, 89 (2007).

[87] J. Schaffner-Bielich and A. Gal, Phys. Rev. C **62**, 034311 (2000).
[88] E. Friedman, A. Gal, and C. J. Batty, Nucl. Phys. A **579**, 518 (1994).
[89] T. Wass and W. Weise, Nucl. Phys. A **625**, 287 (1997).
[90] E. Friedman, A. Gal, J. Mares, and A. Cieply, Phys. Rev. C **60**, 024314 (1999).
[91] A. Baca, C. Garcia-Recio, and J. Nieves, Nucl. Phys. A **673**, 335 (2000).
[92] A. Ramos and E. Oset, Nucl. Phys. A **671**, 481 (2000).
[93] D. Gazda, E. Friedman, A. Gal, and J. Mareš, Phys. Rev. C **77**, 045206 (2008).
[94] T. Waas, M. Rho, and W. Weise, Nucl. Phys. A **617**, 449 (1997).
[95] R. A. Hulse and J. H. Taylor, Astrophys. J. **195**, L51 (1975).
[96] R. A. Chevalier, Astrophys. J. **411**, L33 (1993).
[97] D. J. Nice *et al.*, Astrophys. J. **634**, 1242 (2005).
[98] D. J. Nice, I. H. Stairs, and L. E. Kasianb, AIP Conf. Proc. **983**, 453 (2008).
[99] J. Cottam, F. Paerls, and M. Mendez, Nature **420**, 51 (2002).
[100] T. Rauch, V. Suleimanov, and K. Werner, Astron. Astrophys. **490**, 1127 (2008).
[101] G. Y. Shao, and Y. X. Liu, Phys. Lett. B **682**, 171 (2009).
[102] K. J. Pearson *et al.*, Astrophys. J. **648**, 1169 (2006).
[103] E. F. Brown, L. Bildsten, and R. E. Rutledge, Astrophys. J. **504**, L95 (1998).
[104] R. E. Rutledge, L. Bildsten, E. F. Brown, G. G. Pavlov, and V. E. Zavlin, Astrophys. J. **578**, 405 (2002).
[105] B. Gemdre, D. Barret, and N. A. Webb, Astron. Astrophys. **400**, 521 (2003).
[106] C. O. Heinke, G. B. Rybicki, R. Narayan, and J. E. Grindlay, Astrophys. J. **644**, 1090 (2002).
[107] D. Page and S. Reddy, Annu. Rev. Nucl. Part. Sci. **56**, 327 (2006).